Nanoscale

Accepted Manuscript

Volume 8 | Number 1 | 7 January 2016 | Pages 1–660

Nanoscale

www.rsc.org/nanoscale

ISSN 2040-3364

ROYAL SOCIETY OF CHEMISTRY

PAPER
Qian Wang et al
TiC₂ a new two-dimensional sheet beyond MXenes

NCNST

This is an Accepted Manuscript, which has been through the Royal Society of Chemistry peer review process and has been accepted for publication.

Accepted Manuscripts are published online shortly after acceptance, before technical editing, formatting and proof reading. Using this free service, authors can make their results available to the community, in citable form, before we publish the edited article. We will replace this Accepted Manuscript with the edited and formatted Advance Article as soon as it is available.

You can find more information about Accepted Manuscripts in the author guidelines.

ROYAL SOCIETY OF CHEMISTRY

rsc.li/nanoscale

Nanoscale

ARTICLE

Open-book-like triboelectric nanogenerators based on low-frequency roll-swing oscillator for wave energy harvesting†

Wei Zhong,‡[ab] Liang Xu,‡[ab] Xiaodan Yang,‡[ab] Wei Tang,[ab] Jiajia Shao,[ab] Baodong Chen[ab] and Zhong Lin Wang*[abc]

The invention of triboelectric nanogenerators (TENGs) provides a great opportunity for large-scale harvesting water wave energy that is both clean and renewable. To realize the prospect, devices with high power density and low-frequency response capability are highly desired. Here, an open-book-like triboelectric nanogenerator with boosted power density and high responsivity to wave agitations is presented. The device efficiently integrates a large number of TENG units into an open-book-like structure in a limited space, greatly improving the volume density of microstructured contact interface. A mechanism of force conduction chain is proposed for the first time to effectively drive multiple stacked TENG units. For a device with 50 units, the transferred charges can reach 26 μC and the short-circuit current is 0.45 mA, which should set new records of similar devices. The design of the roll-swing oscillator demonstrates a nonlinear feature in the elasticity with double energy minimums, enabling wide frequency response at low frequencies which is crucial for harvesting wave energy. When agitated by water waves, the roll-swing oscillator can respond effectively to the excitation and drive the stacked TENG units with the assistance of the force conduction chain. A high peak power density of 7.45 W m^{-3} and an average power density of 0.335 W m^{-3} in water were obtained. Such high-performance of the device makes it an excellent candidate for constructing marine self-powered systems or large-scale wave energy harvesting farms to realize the blue energy dream.

Introduction

Developing renewable and clean energy is a critical issue for the sustainable development of human society.[1,2] The ocean covers more than 70% of the surface of the earth. There is a huge amount of energy to be exploited, which is both renewable and clean.[3] Among various types of ocean energies, the wave energy is one of the most focused due to its large amount and wide distribution.[4,5] The technologies to exact water wave energy have been developed for decades, most of which depend on electromagnetic generators (EMGs).[6,7] Due to the requirements of the EMGs on the mechanical structure, the devices are usually large, inefficient and expensive.[4,6,7] Thus it is not wide commercially applied after years of research. Recently, the invention of triboelectric nanogenerators (TENGs) has brought a new opportunity for harvesting water wave energy, where large-scale TENG networks are proposed to be applied.[8-10] The TENG can effectively convert random low-frequency mechanical agitations into electricity, which is especially suitable for wave energy harvesting that is mainly in low-frequency forms.[11] The working mechanism of the TENG is based on the coupling of triboelectrification and electrostatic induction, and its origin can be derived to Maxwell's displacement current.[12] The TENG has the merits of low cost, simple fabrication and versatile choices of materials.[12,13] Since its invention, various types of TENGs have been proposed to harvest energy from human walking, wind, vibration and so on.[14-20] For the harvesting of water waves, several prototypes are presented to verify the principle.[21-26] The most typical device should be the ball-shell structure based on the freestanding triboelectric layer mode, where a solid ball is adopted to roll in a spherical shell.[10,25] An improved device using soft silicone rubber ball is proposed to enhance the charge output by about three times in 2018.[24] Though the ball-shell structure is relatively simple and facile to fabricate, the contact area per volume is relatively low, which limits the output of the device. The design using contact-separation mode can have a larger contact area.[22,26] However, there still needs a more effective method to integrate a large number of units in a limited space and drive them simultaneously to achieve higher power density. Meanwhile, the low-frequency response characteristics that can effectively convert the water waves into the inner motions of the TENGs are not well realized in present devices.[21]

a. CAS Center for Excellence in Nanoscience, Beijing Key Laboratory of Micro-nano Energy and Sensor, Beijing Institute of Nanoenergy and Nanosystems, Chinese Academy of Sciences, Beijing, 100083, China. E-mail: zlwang@binn.cas.cn (Z. L. Wang)
b. School of Nanoscience and Technology, University of Chinese Academy of Sciences, Beijing, 100049, China
c. School of Material Science and Engineering, Georgia Institute of Technology, Atlanta, Georgia, 30332, USA
† Electronic Supplementary Information (ESI) available: Supplementary videos. See DOI: 10.1039/x0xx00000x
‡ W. Zhong, L. Xu, X. Yang contributed equally to this work
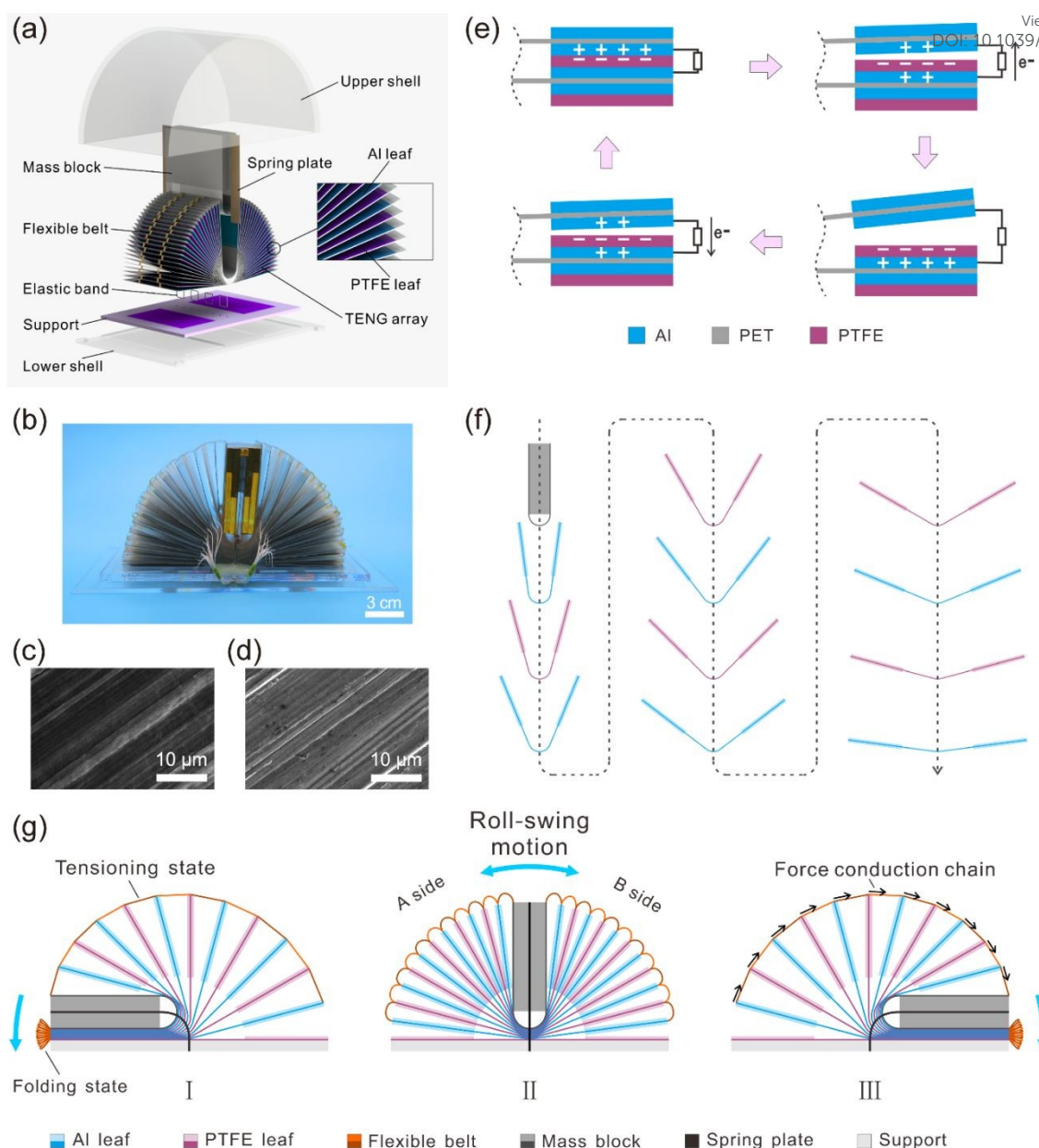
Fig. 1 Structure and working principle of the OB-TENG device. (a) Schematic explosive view of the device. (b) Photograph of the fabricated device. (c, d) SEM images of treated PTFE and Al surfaces, respectively. (e) Working principle of each TENG unit of OB-TENG (not to scale). (f) Schematic diagram of the assembly of leaves and mass block. (g) Schematic illustration of the roll-swing oscillation of the device.

In this work, an open-book structured triboelectric nanogenerator (OB-TENG) based on low-frequency (<< 1 Hz) roll-swing oscillation is presented for wave energy harvesting. The device efficiently integrates a large number of TENG units into an open-book-like structure in a limited space, greatly improving the volume density of the contact interface. A mechanism of force conduction chain is proposed for effectively drive multiple stacked TENG units. For a device with 50 units, the transferred charges can reach 26 μC and the short-circuit current is 0.45 mA. The design of the roll-swing oscillator shows a nonlinear feature in the elasticity with double energy minimums, enabling inherent wide frequency response in low frequencies. When agitated by water waves, the roll-swing oscillator can response effectively to the excitation and drive the stacked TENG units with the assistance of the force conduction chain. A high peak power density of 7.45 W m^{-3} and an average power density of 0.335 W m^{-3} in water were obtained.

Results and discussion

The structure of the OB-TENG is schematically shown in Fig. 1a. There are two major parts in the device, an open-book-like TENG array and a roll-swing oscillator. The open-book-like
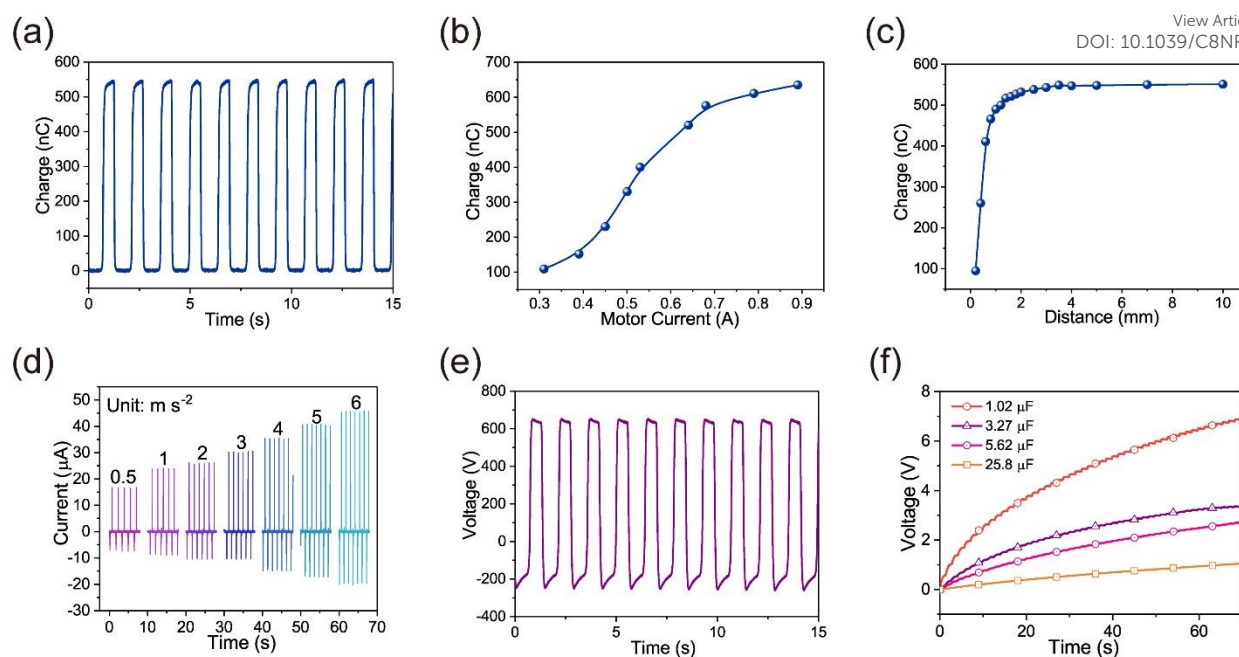
Fig. 2 Output performance of single TENG unit. (a) Transferred charges of single TENG unit. (b, c) Dependence of transferred charges on driving motor current and separation distance, respectively. (d) Short-circuit current with different contact-separation accelerations. (e) Open-circuit voltage of single TENG unit. (f) Charging performance to different capacitors. The separation distance is 10 mm and the acceleration is 1 m s^{-2} unless otherwise specified.

TENG array is composed by an acrylic support and a series of poly(ethylene terephthalate) (PET) sheets, which are referred as leaves and stacked in the way shown in Fig. 1f. There are two types of leaves, namely Al leaves and polytetrafluoroethylene (PTFE) leaves. The Al leaves have Al friction electrodes attached on the PET sheet, and the PTFE leaves have PTFE films and Al back electrodes attached, which form TENG units between each adjacent Al leaf and PTFE leaf. The roll-swing oscillator mainly includes a spring plate and a mass block wrapped in a bare PET leaf, and is mounted on the support from the root of the spring plate. All the PET leaves and the acrylic support are bundled loosely by four elastic bands, and the ends of each adjacent PET leaf are connected by flexible belts to form a force conduction chain as shown in Fig. 1g. The whole structure is sealed by the upper shell and the lower shell that are made of acrylic. Fig. 1b demonstrates a photograph of a fabricated device without the shell. The surfaces of the Al friction electrodes and the PTFE films were brushed with 3000-mesh sandpaper to create microstructures for enhancing the surface contact,[27] and the scanning electron microscope (SEM) images of the treated PTFE and Al surfaces are shown in Figs. 1c and d, respectively.

Fig. 1e explains the working principle of a single TENG unit, which is based on the coupling of tribo-electrification and electrostatic induction.[13,28] Firstly, the Al friction electrode and the PTFE film are in contact state, and positive charges in the Al friction electrode and negative charges on the surface of the PTFE film are generated due to their different affinities to charges. Then as the Al friction electrode and the PTFE film are separated, potential difference is generated between the Al

back electrode of the PTFE film and the Al friction electrode, driving electrons to flow from the Al back electrode to the Al friction electrode to generate a current until they reach the maximum separation. Lastly, when the Al friction electrode approaches the PTFE film again, electrons will flow back from the Al friction electrode to the Al back electrode, producing a reverse current. Thus periodical contact-separation of the Al friction electrode and the PTFE film can produce an alternate periodic current output. In our device, the contact-separation is realized by the roll-swing motion of the oscillator, as shown in Fig. 1g. The arcs of the PET sheets enable roll around the bottoms with swing motion of the upper part. When the oscillator swings to the left by the triggering of water waves, the TENG units on the A side will be compressed to the contact state, and the units on the B side will separate completely through the assistance of the flexible belts in tensioning state, whereas the flexile belts at the A side will be in folding state. When the oscillator swings to the right, the TENG units on the A side will separate and the units on the B side will contact. The elasticity of the spring plate provides a major restoring force to the system under large swing while the elastic bands and PET sheets can also contribute. The spring plate and the mass block form a spring-oscillator-like mechanism that can oscillate with periodic external agitations such as water waves, and it has wide frequency response in low frequencies that is crucial for water wave energy harvesting as will be discussed in details later. We should emphasize the significant role of the flexible belts in the separation of the TENG units. Generally, for multiple stacked TENG units, the force from two ends usually can't separate the TENGs uniformly due to the lack of a force
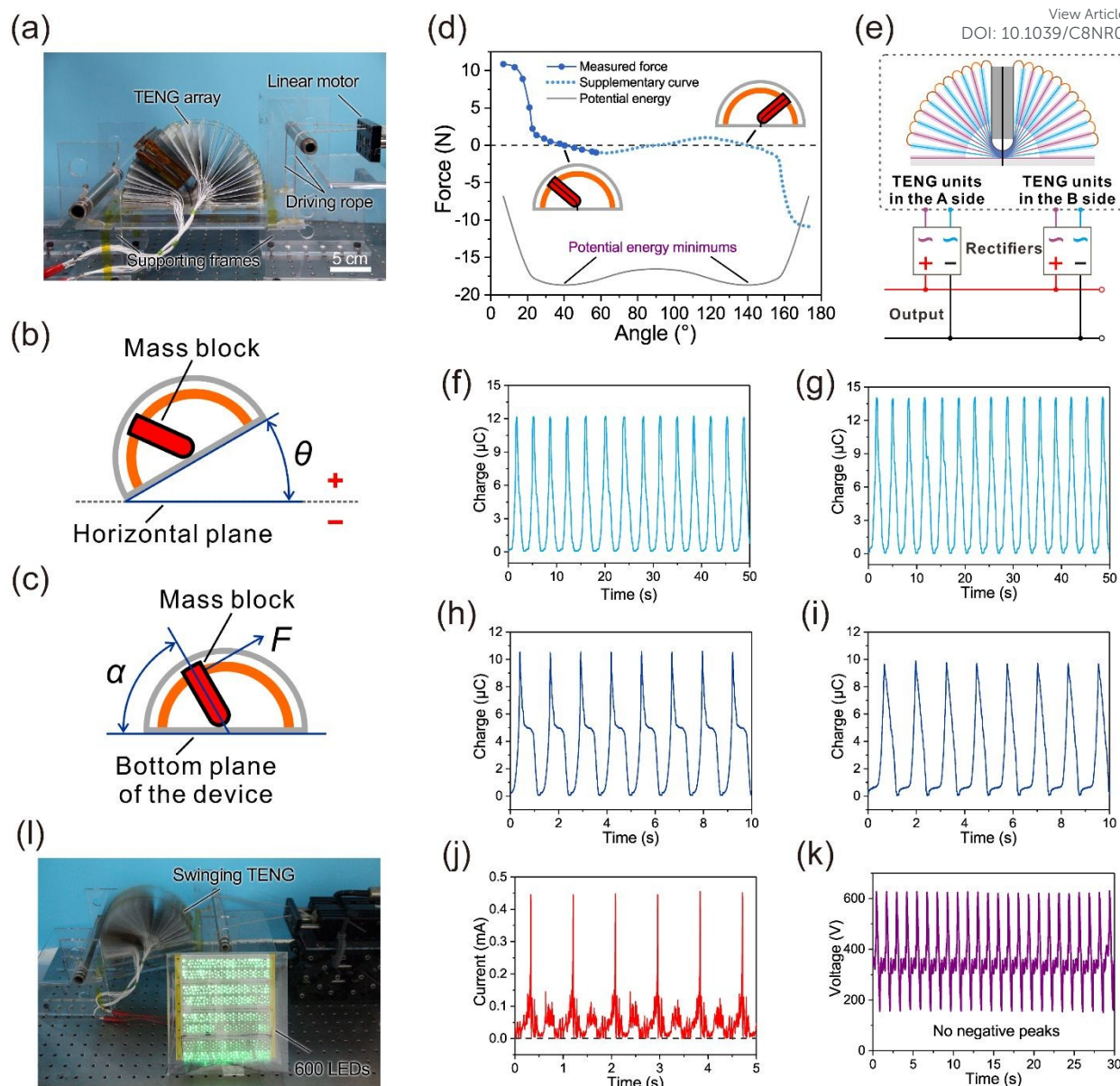
Fig. 3 Basic characterization of the OB-TENG in air. (a) Photograph of the experiment setup. (b, c) Schematic illustration of tilt angle, swing angle and the total force on the mass block. (d) Dependence of the total force on the swing angle and the potential energy minimums of the device. (e) Schematic diagram of the rectification circuit for the device. (f, g) Transferred charges of the A side and B side with ideal compression on the mass block, respectively. (h, i) Transferred charges of the A side and B side with a driving frequency of 0.8 Hz and an amplitude of 13.6°, respectively. (j, k) Rectified short-circuit current and open-circuit voltage of the whole device with a driving amplitude of 13.6°, respectively. (l) Photograph of the swinging TENG and 600 lighted LEDs.

conduction mechanism. Here, the tensioning of the flexible belts in the separation process would form a force conduction chain, which can convey the driving from the oscillator to each leaf and achieve almost uniform separations in each TENG. The flexible belts do not affect the contact state as they can fold up. The design of the OB-TENG enables integration of a large number of TENG units and effective utilization of the space. Compared to the ball-shell structure,[21,24,25] the structure adopts multiple roll-swing leaves to replace the rolling ball, which greatly improves the density of contact interface, thus high output density can be expected. In our experiments, 50

TENG units are integrated into the semi-cylindrical space for demonstration, which can be further augmented to a large extent for fully utilizing the space.

In order to understand the basic output characteristics of the OB-TENG device, we first measured the TENG unit triggered by a linear motor in air. Output performance of a single TENG unit is shown in Fig. 2. The short-circuit transferred charges Q_{SC} and peak open-circuit voltage V_{OC} of the TENG unit reach up to 0.54 μC and 650 V under triggering at a separation distance of 10 mm and an acceleration of 1 m s^{-2} (Figs. 2a and e). The transferred charges rise to a saturation
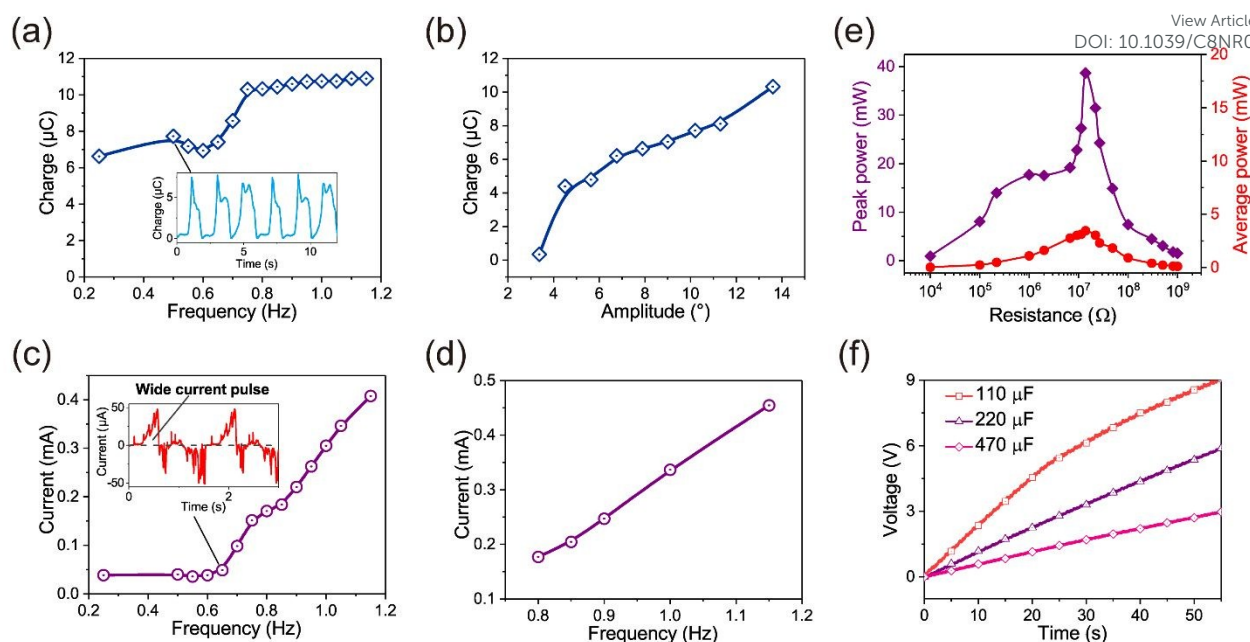
Fig. 4 Electrical output of the OB-TENG in air. (a, b) Dependence of the transferred charges of the A side on different driving frequencies and amplitudes, respectively. Inset: Profile of the output charges. (c) Dependence of the peak short-circuit current of the A side on different driving frequencies. Inset: Profile of the output current. (d) Dependence of the peak rectified short-circuit current of the whole device on different driving frequencies. (e) Average power and peak power of the whole device with different resistive loads by agitations of 1 Hz. (f) Charging performance of the device to different capacitors. The agitation frequency is 0.8 Hz and the amplitude is 13.6° unless otherwise specified.

with increasing separation distance (Fig. 2c) or motor current that is proportional to the compression force at contact (Fig. 2b). The speed of contact-separation increases with larger accelerations, thus higher short-circuit currents I_{SC} were obtained with shorter time for charge transferring (Fig. 2d), consistent with the equation $I_{SC} = dQ_{SC}/dt$. The short-circuit current at 6 m s^{-2} can reach 45 μA. In practical applications, the electrical energy generated by the TENG is usually stored in an energy storage unit such as a capacitor or a battery to provide a stable and controllable power output. The charging performance of the TENG unit to capacitors is shown in Fig. 2f. The charging rate for smaller capacitors is much faster which can reach a relatively high voltage within a short time. Typically, the single TENG unit can charge a 1.02 μF capacitor to 6.5 V in about 60 s.

For the purpose of understanding the response characteristics of the device to regular wave agitations, we first test the device with a self-made tool driven by a linear motor to simulate the agitation of water waves, as shown in Fig. 3a and ESI Video S1 †. The device mounted on the supporting frames can rotate about the axis by the drag of a driving rope that is connected to the linear motor. The state of the device can be defined by two parameters, namely the tilt angle θ between the bottom of the device and the horizontal plane, and the swing angle α between the mass block and the bottom of the device (Figs. 3b, c). We measured the static total force F perpendicular to the mass block at the edge of the oscillator with different swing angles when the tile angle is zero, as shown in Fig. 3d. The curve is supplemented according

to the symmetry of the device. The total force is basically composed by the restoring force of the spring plate and the gravity effect of the mass block, and two zero-force angles can be observed at 40.3° and 139.7°. The potential energy of the system E_P is related to the force according to the equation:

$$E_P = \int F dl \qquad (1)$$

where dl is the displacement of the edge along the direction of the force. A schematic curve of the potential energy is demonstrated in Fig. 3d. There are two local energy minimums in the whole range of the swing angle from about 0° to 180°, corresponding to the two zero-force angles, which is different from linear spring-oscillator systems where only one potential energy minimum exists. Without external agitations, the mass block would reside at one of these two swing angles when the tilt angle is zero. The force plot and the double energy minimums show the nonlinear nature of the system where wide frequency response in low frequencies can be expected, and the relative large mass and low effective stiffness near potential energy minimums contribute to the low-frequency characteristics.

Before testing the electrical output of the device, we designed a rectification circuit as shown in Fig. 3e. Because the TENG units from different sides have a phase mismatch according to the working mechanism, the TENG units in the A side and the B side are rectified respectively by two rectifiers before being parallel connected for combined output. The charge output is crucial for the performance of TENG. We tested first the maximum transferred charges by fully
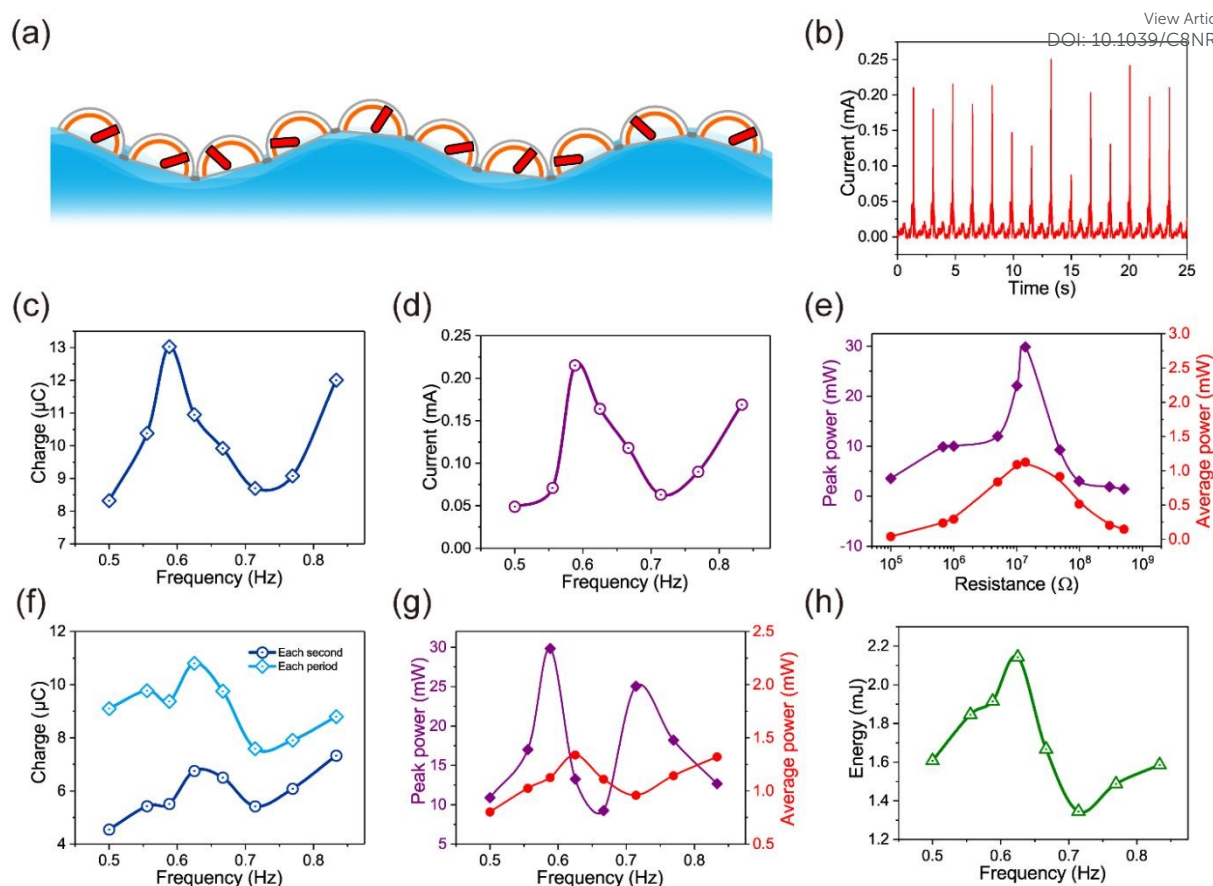
Fig. 5 Output performance of the device in water. (a) Schematic illustration of working principle of the device in water. (b) Profile of the rectified short-circuit current of the device in water. (c, d) Dependence of the transferred charges and rectified short-circuit current of the whole device on different wave frequencies. (e) Power output of the whole device in water with different resistive loads. (f) Transferred charges of the device in each period and each second for different wave frequencies with the matched load of 13.8 MΩ. (g) Average power and peak power for different frequencies with the matched load of 13.8 MΩ. (h) Output energy in each period for different frequencies with the matched load of 13.8 MΩ. The frequency of the water wave is 0.588 Hz unless otherwise specified.

compressing the TENG units. The short-circuit transferred charges of the A side and the B side can reach 12 μC and 14 μC respectively (Figs. 3f and g), which are much larger than previously reported devices.[21] Compared to the ball-shell structured device with a diameter of 6 cm,[25] the total charge output is enhanced by over 1000 times while the volume is only about 36 times. For normal harmonic agitations with the linear motor at a frequency of 0.8 Hz and an amplitude of 13.6°, the transferred charges are 10.5 μC and 9.8 μC respectively (Figs. 3h and i), indicating that the oscillator can well respond to low-frequency agitations and efficiently drive the TENG units. The rectified short-circuit current of the whole device can reach up to 0.45 mA at a frequency of 1.15 Hz and an amplitude of 13.6° (Fig. 3j). The rectified open-circuit voltage peaks at 625 V for a driving frequency of 0.8 Hz (Fig. 3k). As an intuitive demonstration of the output of the device, 600 light-emitting diodes (LEDs) can be lighted directly by the swinging TENG, as shown in Fig. 3l.

We further characterized the response of the device to external harmonic agitations with different frequencies and amplitudes. Considering the symmetry of the device, we present the charge output of the A side in Figs. 4a and b. The transferred charges of the A side show an increasing trend with higher frequencies. It first reaches a local maximum at about 0.5 Hz, then rise rapidly in the range of 0.65 Hz and 0.75 Hz to achieve a slow-augmenting plateau from 0.75 Hz, demonstrating good response to a wide frequency range in low frequencies. Such characteristics should be attributed mainly to the nonlinear feature of the system as discussed above. For the amplitude, the charge output increases monotonically with rising amplitude which imposes stronger agitations to the device. The short-circuit current of the device in response to different agitation frequencies is shown in Fig. 4c. The current peak rises fast with the frequencies higher than 0.65 Hz, which has much higher charge output and lower period, consistent with the equation $I_{SC} = dQ_{SC}/dt$. There is also a small local maximum at 0.5 Hz. The profile of the current output shows wide current pulses which should be composed by the currents of multiple TENG units, different from normal contact-separation device where only very narrow current
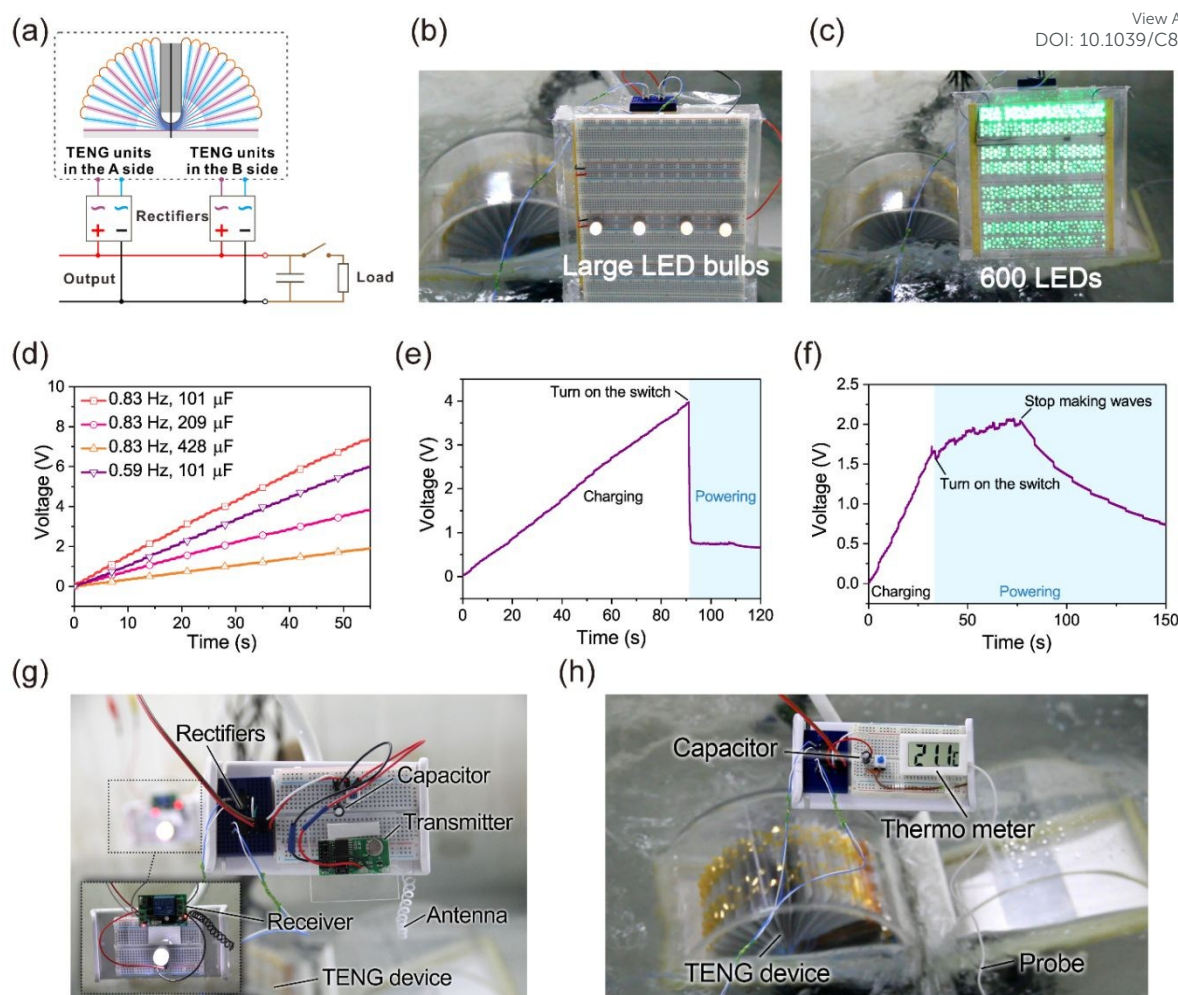
Fig. 6 Demonstrations of the wave-agitated OB-TENG powering electrical loads. (a) Circuit diagram of the OB-TENG connected to the load. (b, c) Photographs of the OB-TENG lighting 4 large LED bulbs and 600 LEDs, respectively. (d) Charging performance of the wave-agitated device to different capacitors. (e, f) Charging and discharging processes for powering a wireless transmitter and a thermo meter, respectively. (g, h) Photographs of driving the wireless transmitter and the thermo meter with the wave-agitated OB-TENG. The frequency of the water wave is 0.588 Hz unless otherwise specified.

pulse can be observed.[28] The total current output of the whole device is shown in Fig. 4d. Comparing with the current of the A side, the current peak is enhanced a bit but not doubled. The power output of the device with different resistive loads is presented in Fig. 4e. A peak power of 38.7 mW and an average power of 3.45 mW were obtained at a matched resistance of 13.8 MΩ. Considering the device has a volume of 0.004 m^3, the peak power density and the average power density can reach 9.675 W m^{-3} and 0.863 W m^{-3} respectively, indicating high performance of the device in harvesting low-frequency energy. The power density can be further improved because the inner space can accommodate much more TENG units than 50. The nontrivial profile of the peak power should originate from the unsynchronized contact-separation of multiple TENG units in the device that can produce enhanced peak current in some conditions. Fig. 4f shows the charging performance of the whole device to different capacitors, which can quickly reach a voltage that is enough to drive small electronic devices.

To test the performance of the device in real water circumstance, wave tank experiments were conducted. The water waves were generated by nine wave makers that were controlled by a function generator. The working mechanism of the device in water is briefly illustrated in Fig. 5a. A series of single OB-TENG devices is interconnected to form a network. Through the network coupling effect,[24] the OB-TENGs can be effectively agitated by the water waves. In our experiments, the OB-TENG device was connected to a model device that has the same shell shape with the OB-TENG to compose the simplest network. Two extra masses (977 g) were attached to the bottom of the two shells at the connected side to provide a restoring force considering that the network only has two components. The amplitude of the signal to drive the pump is constant in our tests, and the influence of the frequency on the output of the device is mainly discussed. Fig. 5b shows typical current output of the device in water, and a peak rectified current of more than 0.22 mA can be achieved at a

Nanoscale Accepted Manuscript

wave frequency of 0.588 Hz. The dependence of the total transferred charges and the peak rectified current of the device on the wave frequency is shown in Figs. 5c and d. There are local maximums at 0.588 Hz for the charge and the current output, reaching 13 μC and 0.22 mA respectively, and an output enhancement beyond 0.71 Hz can also be observed. Such behavior is similar with the frequency response agitated by linear motor which can also be attributed to the nonlinear feature of the device. The agitation of water waves is more complicated than the harmonic agitation, thus the results show some differences in the position and height of local maximums. The charge output is smaller than that driven by the linear motor, indicating that the device was not fully agitated which can be further improved by a better wave environment. Fig. 5e presents the power output of the device in water, a peak power of 29.8 mW and an average power of 1.13 mW can be delivered at the matched load resistance of 13.8 MΩ under wave frequency of 0.588 Hz, corresponding to a peak power density of 7.45 W m^{-3} and an average power density of 0.283 W m^{-3}. We investigated the charge, power and energy output of the device with the load of 13.8 MΩ at different wave frequencies, as shown in Figs. 5f-h. The variation of the charge output per period (or per second), the average power and the energy output per period show a high correlation, whereas the peak power has very different features. At the local maximum of 0.625 Hz, the output energy per period is 2.14 mJ, and the average power reaches 1.34 mW, corresponding to an average power density of 0.335 W m^{-3}. The above results show that the OB-TENG can be effectively agitated by low-frequency water waves owing to the inherent low-frequency-response capability of the device, and the power output is greatly enhanced compared with previous works, where an improved ball-shell structured device can output a peak power of 1 mW under agitations of 3 Hz.[21,24,25]

With the excellent water wave energy harvesting performance, the OB-TENG can be adopted to fabricate self-powered systems.[12,29] Here, a few demonstrations are presented. Fig. 6a shows the application circuit where a capacitor can be applied in some situations to store the energy for relative high power applications. Figs. 6b and c demonstrate that the OB-TENG can light directly 4 large LED bulbs or 600 LEDs that are connected to the total rectified output of the device driven by water waves (Also shown in ESI Video S2 †). The charging performance of the device to different capacitors is presented in Fig. 6d. With the stored energy in capacitors, the OB-TENG is able to drive small electronic devices. Figs. 6e, g and and ESI Video S3† show a demonstration that uses the device to power wireless transmission. After charging a capacitor of about 220 μF for 91 s, the voltage reached 3.97 V and the switch was closed. The transmitter was powered by the harvested energy and sent a signal to the receiver to turn on a LED bulb. Here, the transimission distance is about 1.5 m as a demonstration. For practical applications with larger distance, more energy is needed, thus a longer charging time is required. Another demonstration is a self-powered temperature-sensing system,

as shown in Figs. 6f, h and ESI Video S4 †. The capacitor of about 220 μF was initially charged to 1.65 V within 33 s. The switch was then closed to power a thermo meter to measure the temperature of the water. The thermo meter could be powered continuously by the OB-TENG until the wave maker stopped, as shown in Fig. 6f. As an effective structure for water wave energy harvesting, the OB-TENG can also be integrated into other shapes of shells, such as in a hollow ball structure for specific demands. We expect that the device can be applied to construct ocean sensory platform for self-powered marine monitoring. Large-scale networks of the device can produce enough electricity to be transferred to small islands or the land to supply power for the electricity grid, providing a renewable and clean energy source.[10]

Conclusions

In summary, an open-book structured triboelectric nanogenerator based on low-frequency (<< 1 Hz) roll-swing oscillation for wave energy harvesting is demonstrated. The device can efficiently integrate a large number of TENG units into an open-book-like structure in a limited space, greatly improving the volume density of the contact interface. A mechanism of force conduction chain is proposed for effectively drive numerous stacked TENG units. For a device with 50 units, the transferred charges can reach 26 μC and the short-circuit current is 0.45 mA. The charge output is over 1000 times compared with typical ball-shell structured device.[25] The design of the roll-swing oscillator demonstrates a nonlinear feature in the elasticity with double energy minimums, enabling inherent wide frequency response in low frequencies, which is highly desired for water wave energy harvesting. When agitated by low-frequency water waves, the roll-swing oscillator can response effectively to the excitation and drive the multiple stacked TENG units with the assistance of the force conduction chain. A high peak power density of 7.45 W m^{-3} and an average power density of 0.335 W m^{-3} in water were obtained. Moreover, it is demonstrated to continuously power a thermo meter. Such high-performance enables the OB-TENG to be an excellent candidate for constructing marine self-powered systems or large-scale wave energy harvesting farms to realize the blue energy dream.

Experimental

Fabrication of the leaves

25 pieces of PET sheets (0.3 mm in thickness) were cut by a laser cutter with dimensions of 180 mm × 100 mm, and eight circular holes (4 mm in diameter) were cut in the center of each sheet. The PET sheets were then hot-bent into a leaf-like structure with even-distributed angles as shown in Fig. 1f. Al friction electrodes (100 mm × 60 mm) and PTFE films (80 μm in thickness) with Al back electrodes (100 mm × 60 mm) were attached to the corresponding leaves by pressure-sensitive adhesive in both sides. The acrylic support plate (6 mm in thickness) with dimensions of 210 mm × 150 mm was

prepared by the laser cutter, and eight circular holes and two strip holes were cut in the center of the plate. PTFE films with Al back electrodes were attached to the upper side of the support by pressure-sensitive adhesive. The surfaces of the Al friction electrodes and the PTFE films were treated with 3000-mesh sandpaper, and the PTFE films were corona charged with a voltage of 6.5 kV for 5 minutes. Another piece of PET sheet with the same dimensions and a thickness of 1mm were hot-bent to an angle of 0° for encapsulating the mass block.

Fabrication of the OB-TENG

All the prepared PET sheets were stacked in order and bundled to the support through the eight circular holes with elastic bands. A mass block (811 g) is fixed to a 0.3 mm thick steel spring plate (65Mn) from the upper end and encapsulated by the 1 mm thick PET sheet. Then the two legs of the spring plate were inserted into the two strip holes in the support plate and fixed by adhesive. The ends of each adjacent PET sheet were connected by flexible polyimide belts. The whole structure was then packaged by acrylic shells and the support was fixed on the lower shell.

Device characterization

The output charge and current of the TENG and the voltage of the capacitor were measured by an electrometer (Keithley 6514). The open-circuit voltage of the TENG was measured by an electrostatic voltmeter (Trek 344) to detect the potential of the electrode. The force was measured by a load cell (FUTEK LRM200-10lb).

Conflicts of interest

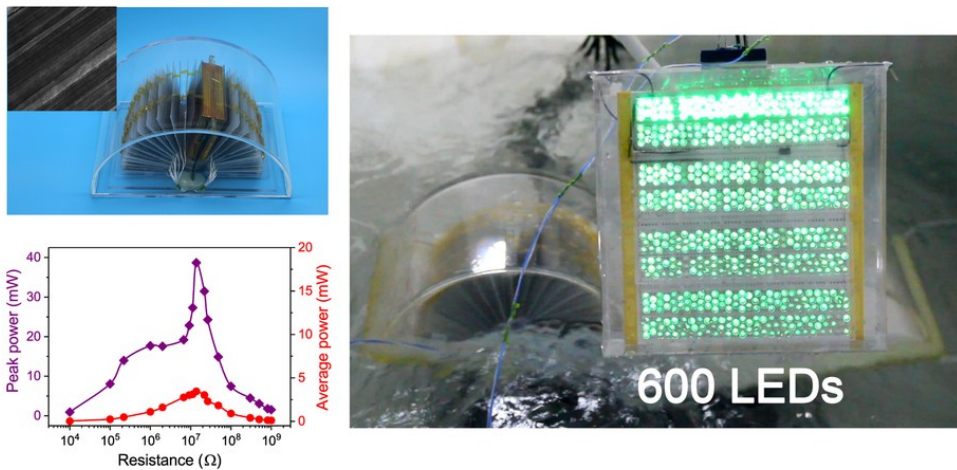There are no conflicts to declare.

Acknowledgements

References

1   Q. Schiermeier, J. Tollefson, T. Scully, A. Witze and O. Morton, *Nature*, 2008, **454**, 816-823.
2   D. Gielen, F. Boshell and D. Saygin, *Nat. Mater.*, 2016, **15**, 117-120.
3   J. Tollefson, *Nature*, 2014, **508**, 302-304.
4   E. Callaway, *Nature*, 2007, **450**, 156-159.
5   J. Scruggs and P. Jacob, *Science*, 2009, **323**, 1176-1178.
6   B. Drew, A. R. Plummer and M. N. Sahinkaya, *P. I. Mech. Eng. A-J. Pow.*, 2016, **223**, 887-902.
7   A. F. d. O. Falcão, *Renew. Sust. Energy Rev.*, 2010, **14**, 899-918.
8   F.-R. Fan, Z.-Q. Tian and Z. Lin Wang, *Nano Energy*, 2012, **1**, 328-334.
9   Z. L. Wang, *Faraday discuss.*, 2014, **176**, 447-458.
10   Z. L. Wang, *Nature*, 2017, **542**, 159-160.
11   Y. Zi, H. Guo, Z. Wen, M. H. Yeh, C. Hu and Z. L. Wang, *ACS Nano*, 2016, **10**, 4797-4805.
12   Z. L. Wang, *Mater. Today*, 2017, **20**, 74-82.
13   S. Niu and Z. L. Wang, *Nano Energy*, 2015, **14**, 161-192.
14   Z. L. Wang, J. Chen and L. Lin, *Energy Environ. Sci.*, 2015, **8**, 2250-2282.
15   G. Zhu, B. Peng, J. Chen, Q. Jing and Z. Lin Wang, *Nano Energy*, 2015, **14**, 126-138.
16   S. Niu, X. Wang, F. Yi, Y. S. Zhou and Z. L. Wang, *Nature Commun.*, 2015, **6**, 8975.
17   J. Wang, S. Li, F. Yi, Y. Zi, J. Lin, X. Wang, Y. Xu and Z. L. Wang, *Nature Commun.*, 2016, **7**, 12744.
18   J. Bae, J. Lee, S. Kim, J. Ha, B. S. Lee, Y. Park, C. Choong, J. B. Kim, Z. L. Wang, H. Y. Kim, J. J. Park and U. I. Chung, *Nature Commun.*, 2014, **5**, 4929.
19   L. Xu, T. Z. Bu, X. D. Yang, C. Zhang and Z. L. Wang, *Nano Energy*, 2018, **49**, 625-633.
20   J. Xiong, P. Cui, X. Chen, J. Wang, K. Parida, M. F. Lin and P. S. Lee, *Nature Commun.*, 2018, **9**, 4280.
21   Z. L. Wang, T. Jiang and L. Xu, *Nano Energy*, 2017, **39**, 9-23.
22   L. Xu, Y. K. Pang, C. Zhang, T. Jiang, X. Y. Chen, J. J. Luo, W. Tang, X. Cao and Z. L. Wang, *Nano Energy*, 2017, **31**, 351-358.
23   G. Zhu, Y. Su, P. Bai, J. Chen, Q. Jing, W. Yang and Z. L. Wang, *ACS Nano*, 2014, **8**, 6031-6037.
24   L. Xu, T. Jiang, P. Lin, J. J. Shao, C. He, W. Zhong, X. Y. Chen and Z. L. Wang, *ACS Nano*, 2018, **12**, 1849-1858.
25   X. F. Wang, S. M. Niu, Y. J. Yin, F. Yi, Z. You and Z. L. Wang, *Adv. Energy Mater.*, 2015, **5**, 1501467.
26   J. Chen, J. Yang, Z. L. Li, X. Fan, Y. L. Zi, Q. S. Jing, H. Y. Guo, Z. Wen, K. C. Pradel, S. M. Niu and Z. L. Wang, *ACS Nano*, 2015, **9**, 3324-3331.
27   L. Zhao, Q. Zheng, H. Ouyang, H. Li, L. Yan, B. Shi and Z. Li, *Nano Energy*, 2016, **28**, 172-178.
28   S. Niu, S. Wang, L. Lin, Y. Liu, Y. S. Zhou, Y. Hu and Z. L. Wang, *Energy Environ. Sci.*, 2013, **6**, 3576.
29   W. Tang, Y. Han, C. B. Han, C. Z. Gao, X. Cao and Z. L. Wang, *Adv. Mater.*, 2015, **27**, 272-276.

Open-book-like triboelectric nanogenerator enables highly effective wave energy harvesting with boosted power and charge output for self-powered marine systems.

Nanoscale Accepted Manuscript

79x39mm (300 x 300 DPI)